G-014

A Registration Between 3D Ultrasound Images and 3D Fetal Model for Locating a Fetal Mouth in a Fetal Surgical Navigation System

Rong Xu[1], Jun Ohya[1], Bo Zhang[2], Yoshinobu Sato[3], Masakatsu G. Fujie[2]

1. Introduction

Congenital diaphragmatic hernia (CDH) is a severe defect, has a prevalence of 1 in 2,000-3,000 newborns. The outcome of fetuses with CDH may be improved by fetal endoscopic tracheal occlusion (FETO) with a balloon, and a minimally invasive surgery (MIS) is operated for FETO to position a balloon into fetal trachea by the navigation of 2D ultrasound images and fetoscopic images [1, 2]. This surgery is so difficult that autonomous surgical supporting systems (for inserting a surgical tool into fetal mouth and trachea) are desired to be actualized.

3D ultrasound (US) images are very useful for FETO surgery, but due to speckle noise, shadows, attenuation, signal dropout and low resolution, the anatomy of fetal oral cavity and airways cannot be distinguished clearly from 3D US images, as shown in Fig. 2 (a). On the other hand, the anatomy of fetal airways can be visualized by MR or CT images; however, no work on the reconstruction of 3D model with fetal airways from MRI or CT can be seen, and also there is no available product of 3D fetal model with fetal airways at present. In this paper, we reconstruct such a 3D fetal model, and register it with the extracted 3D surface of a fetal face from 3D US images by iterative closet point (ICP) algorithm, and help localize the position of fetal oral cavity and airways for FETO surgery. First of all, one point cloud is extracted from 3D fetal model, and another point cloud is extracted from 3D US image by the edge detection we propose in this paper. Then through the registration, the anatomy of fetal oral cavity and airways in 3D fetal model, which cannot be distinguished clearly by 3D US image, can be visualized and localized in 3D US space.

2. 3D Fetal Model

The surface of 3D fetal model is created by scanning a fetal phantom with an untouched high-speed 3D scanner - 3030RGB /MS, as shown in Fig. 1 (a). First, the phantom is made to stand in the front of the scanner. Next, the rotating platform with the phantom rotates a complete circle, and each turn is set to 10°. Then, we can reconstruct a 3D fetal surface by a point cloud data obtained from the untouched 3D scanner in Fig. 1 (b).

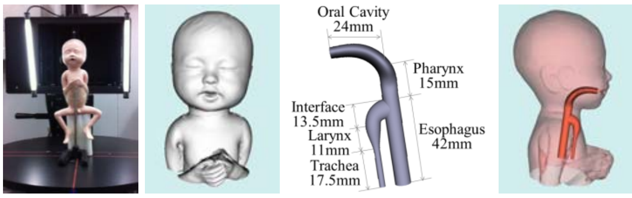

(a) (b) (c) (d)

Fig. 1. 3D fetal model. (a) fetal phantom, (b) 3D fetal surface, (c) the design of fetal oral cavity and airways, (d) 3D fetal model with oral cavity and airways.

There are three parts in the anatomy of fetal oral cavity and airways: (1) oral cavity and pharynx; (2) larynx and trachea; (3) esophagus. Because the FETO surgery is operated at about 26-29 weeks gestational age (GA) [1], thus we select the average size for each part at about 23-29 weeks GA. These structures [3, 4] are drew by Solidworks 2008. To simplify the design, the cross sectional shapes of all tracts are considered as ellipse or circle. The size of each part has been marked out in Fig. 1 (c) based on the reference values in [5-9]. Through the rotation and translation in 3D space, we can obtain a 3D fetal model with fetal oral cavity and airways, as shown in Fig. 1 (d).

3. 3D Rigid Registration

3.1 3D Fetal Surface Extraction

In experiments, we scan a fetal phantom made by silicone resin in a water tank, via a Philips iU22 US system with a V6-2 3D US probe to obtain 3D US images, as shown in Fig. 2 (a).

As we know, unlike MR or CT imaging technology, 3D US image does not have high resolution, as well as the transmission and reflection of ultrasound are easily affected by phantom material and air bubbles in water. Therefore, it is difficult to achieve a 3D US image with clear boundaries of fetal face surface. Owing to the low contrast of 3D US data, we select the slices on X-Y plane from $Z = 100$ to $Z = 170$ with relative clear edges of fetal face surface. In Fig. 2, (a) is a 3D fetal US image, (b) is the extracted slice of $Z = 130$. According to these slices, we find there is just front half of 3D fetal face surface in 3D US data, and accordingly our object is to extract this part from 3D US data. The processing of 3D fetal face surface extraction is described in the following steps and Fig. 2. Here, we take the extracted slice of $Z = 130$ as an example in Fig. 2.

Step 1 The boundaries of the 2D US slice are detected by canny edge detection, as shown in Fig. 2 (c).

Step 2 The ellipse is detected from Fig. 2 (c) by an improved iterative randomized Hough transform proposed in [10]. Then we get five standard parameters $[x_0, y_0, a, b, \phi]$ of the detected ellipse. Based on these parameters, we can estimate a region of interest (ROI) as a rectangle, where the center of this rectangle is set to the center of the ellipse (x_0, y_0), the width and height of this rectangle are set to $a \times 1.1 \times 2$ and $b \times 1.1 \times 2$. Because there is no boundary at the back of fetal head in US data, the ROI is moved up slight (here, we move it up by 50 pixels) in order to be applied for all selected slices, as shown in Fig. 2 (d).

Step 3 The area in the ROI is selected as shown in Fig.2 (e), and then is thresholded into Fig. 2 (f).

Step 4 The pixels in the fetal face surface in Fig. 2 (g) are separated as the largest connected region by a label filter (itk::LabelShapeKeepNObjectsImageFilter) in [11].

Step 5 Binary morphologic closing and opening are operated to smooth the binary result in Fig. 2 (h).

Step 6 The smoothed result in Fig. 2 (h) is scanned from top to bottom, left to right and right to left, and then the red edge of the fetal face in Fig. 2 (i) is distinguished.

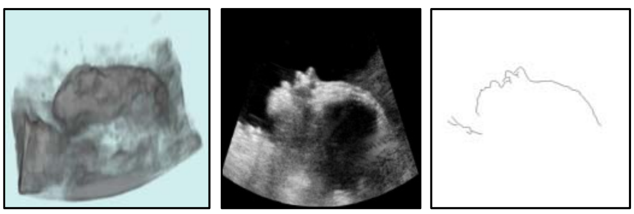

(a) 3D US Image (b) Extracted slice (c) Detected edge

1 Graduate School of Global Information and Telecommunication Studies, Waseda University.
2 Faculty of Creative Science and Engineering, Waseda University.
3 Graduate School of Medicine, Osaka University.

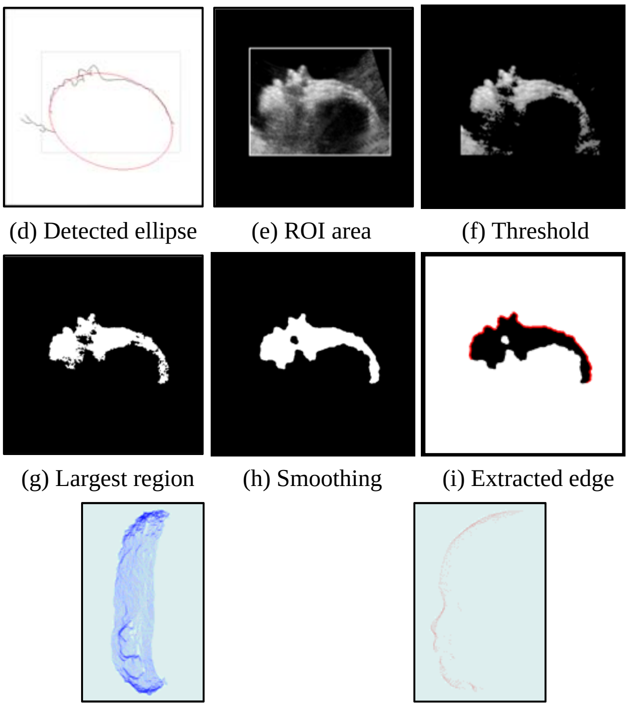

(d) Detected ellipse (e) ROI area (f) Threshold

(g) Largest region (h) Smoothing (i) Extracted edge

(j) 3D point cloud (3D US) (k) 3D point cloud (3D fetal model)

Fig. 2. 3D surface extraction from 3D US image

Step 7 Repeat the steps from (3) to (6) on the slices from *Z = 100* to *Z = 170*, then we can extract a 3D point cloud of fetal face surface, as shown in Fig. 2 (j).

Moreover, another 3D point cloud of the 3D fetal model is extracted by simply setting the range on X, Y and Z axis, as shown in Fig. 2 (k).

3.2 Iterative Closest Point

The iterative closet point (ICP) algorithm for the registration of 3D point clouds was proposed by Yang & Medioni [12] and Besl & McKay [13], which has been widely used in a variety of fields such as medical images, because of its good accuracy and fast speed. Given two point clouds $A = \{a_i\}$ with N_a points, and $B = \{b_i\}$ with N_b points, the transformation of the data A and the data B is assumed to be linear with a rotation matrix T and translation vector r. The goal of the ICP algorithm is to find the transformation parameters, for minimizing the error (mostly least squares) between the transformed data B and the closet points of the data A, which is described by Eq.1.

$$(T, r) = \underset{T,r}{arg\,min} \left(\sum_{i=1}^{N_b} ||a_{c(i)} - (Tb_i + r)||^2\right) \qquad (1)$$

Therefore, we can obtain the transform matrix including rotation and translation from the rigid registration of two point clouds by the ICP algorithm. The registration result is shown in Fig. 3 (a), where the left red source point cloud (containing 3936 points) is extracted from 3D fetal model, the right blue target point cloud (containing 28467 points) is extracted from 3D US image, and the right green resulting point cloud is transformed from the left red source point cloud by the transform matrix. The root mean square (RMS) of the registration result is 3.92 pixels. Besides, we have considered the scale factors on each axis for the transformation between the different coordinate systems.

Based on the estimated transform matrix, we can transform the whole points of the 3D fetal model with oral cavity and airways into 3D US space. The results in Fig. 3 (c) illustrate that the transformed 3D fetal model coincides very well with 3D US image. Then, we can easily confirm the position of fetal oral cavity and airways from the results in Fig. 3 (c).

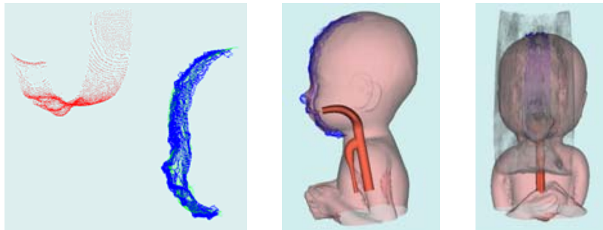

(a) (b) (c)

Fig. 3. The rigid registration of two point clouds

4. Conclusions

In this paper, we realize the rigid registration of two point clouds by the ICP algorithm for FETO surgery, where one point cloud is extract from the 3D fetal model with oral cavity and airways we reconstructed, and another point cloud is extracted from 3D ultrasound image. Through the registration, we can easily confirm the position of fetal oral cavity and airways in 3D ultrasound space, which are difficult to directly be distinguished by 3D ultrasound data. The experimental results demonstrate the registration between 3D fetal model and 3D ultrasound image is quite reliable for visualizing the position of fetal oral cavity and airways in 3D ultrasound space. In the future, we will introduce a 3D ultrasound calibration system to localize the position of fetal oral cavity and airways accurately.

Reference

[1]J. Jani, *et al.*, "Severe diaphragmatic hernia treated by fetal endoscopic tracheal occlusion," *Ultrasound in Obstetrics & Gynecology*, vol. 34, no. 3, pp. 304-310 (2009).

[2]C.A. Hajivassiliou, *et al.*, "Evolution of a percutaneous fetoscopic access system for single-port tracheal occlusion," *Journal of pediatric surgery*, vol. 38, no. 1, pp. 45-50 (2003).

[3]K.L. Moore, *et al.*, *The developing human: clinically oriented embryology*: Saunders (1998).

[4]D. Levine, *Atlas of fetal MRI*: Taylor & Francis (2005).

[5]T.H. Shawker, *et al.*, "Soft tissue anatomy of the tongue and floor of the mouth: an ultrasound demonstration," *Brain and language*, vol. 21, no. 2, pp. 335-350 (1984).

[6]S. Tez, *et al.*, "Ultrasound evaluation of the normal fetal pharynx," *Early human development*, vol. 81, no. 7, pp. 629-633 (2005).

[7]J.L. Miller, *et al.*, "Emergence of oropharyngeal, laryngeal and swallowing activity in the developing fetal upper aerodigestive tract: an ultrasound evaluation," *Early human development*, vol. 71, no. 1, pp. 61-87 (2003).

[8]K.D. Kalache, *et al.*, "Ultrasound measurements of the diameter of the fetal trachea, larynx and pharynx throughout gestation and applicability to prenatal diagnosis of obstructive anomalies of the upper respiratory–digestive tract," *Prenatal diagnosis*, vol. 19, no. 3, pp. 211-218 (1999).

[9]P.C. Brugger, *et al.*, "Magnetic resonance imaging of the normal fetal esophagus," *Ultrasound in Obstetrics & Gynecology*, vol. 38, no. 5, pp. 568-574 (2011).

[10]R. Xu, *et al.*, "Automatic Fetal Head Detection on Ultrasound Images by An Improved Iterative Randomized Hough Transform," In *Processings of 26th International Conference of Image and Vision Computing New Zealand*, Auckland, pp. 288-292 (2011).

[11]G. Lehmann, "Label object representation and manipulation with ITK," *The Insight Journal*, pp. 1-34 (2008).

[12]C. Yang and G. Medioni, "Object modelling by registration of multiple range images," *Image and Vision Computing*, vol. 10, no. 3, pp. 145-155 (1992).

[13]P.J. Besl and N.D. McKay, "A method for registration of 3-D shapes," *IEEE transactions on pattern analysis and machine intelligence*, vol. 14, no. 2, pp. 239-256 (1992).